Nonclassical monocytes are prone to migrate into tumor in diffuse large B-cell lymphoma

Simon Le Gallou,[#,1,2] Faustine Lhomme,[#,1,3] Jonathan M. Irish,[3,4] Anna Mingam,[1] Celine Pangault,[1,2] Celine Monvoisin,[2] Juliette Ferrant,[2] Imane Azzaoui,[1] Delphine Rossille,[1,2] Krimo Bouabdallah,[5] Gandhi Damaj,[6] Guillaume Cartron,[7] Pascal Godmer,[8] Steven Le Gouill,[9] René-Olivier Casasnovas,[10] Thierry Jo Molina,[11] Roch Houot,[2,12] Thierry Lamy,[2,12] Karin Tarte,[1,2] Thierry Fest,[1,2] and Mikael Roussel[1,2]

[1] Centre Hospitalier Universitaire de Rennes, Pôle Biologie, Rennes, France;
[2] Institut national de la santé et de la recherche médicale, Unité Mixte de Recherche U1236, Université Rennes 1, Etablissement Français du Sang Bretagne, Rennes, France;
[3] Department of Cell and Developmental Biology, Vanderbilt University School of Medicine, Nashville, TN, USA;
[4] Department of Pathology, Microbiology and Immunology, Vanderbilt University School of Medicine, Nashville, TN, USA;
[5] Centre Hospitalier Universitaire de Bordeaux, Service d'Hématologie Clinique, Bordeaux, France;
[6] Centre Hospitalier Universitaire de Caen, Service d'Hématologie Clinique, Caen, France;
[7] Centre Hospitalier Universitaire de Montpellier, Service d'Hématologie Clinique, Montpellier, France;
[8] Centre Hospitalier de Bretagne Atlantique, Unité d'Hématologie Clinique, Vannes, France;
[9] Centre Hospitalier Universitaire de Nantes, Service d'Hématologie Clinique, INSERM CCRCINA Nantes-Angers, NeXT Université de Nantes, Nantes, France;
[10] Centre Hospitalier Universitaire de Dijon, Service d'Hématologie Clinique, Dijon, France
[11] APHP, Necker, Service d'Anatomopathologie, Sorbonne Université, Paris, France
[12] Centre Hospitalier Universitaire de Rennes, Service d'Hématologie Clinique, Rennes, France

[#]S.L.G. and F.L. contributed equally to this study.

Correspondence to Mikael Roussel, Laboratoire Hématologie, CHU Pontchaillou, 2 rue Le Guilloux, 35033 Rennes, France; e-mail: mikael.roussel@chu-rennes.fr. Tel.:+33 299 289 142

Running title: Nonclassical monocytes in DLBCL

Word count in abstract: 136
Word count in text: 3603
Figure count: 5
Table count: 1
Reference count: 43

Key points

- Nonclassical monocytes are prone to migrate to DLBCL tumor
- High count of circulating nonclassical monocytes is an independent adverse event in DLBCL

Abstract

Absolute count of circulating monocytes has been proposed as an independent prognostic factor in diffuse large B-cell lymphoma (DLBCL). However, monocyte nomenclature includes various subsets with pro-, anti-inflammatory, or suppressive functions, and their clinical relevance in DLBCL has been poorly explored. Herein, we broadly assessed circulating monocyte heterogeneity in 91 DLBCL patients. Classical- (cMO, $CD14^{pos}$ $CD16^{neg}$) and intermediate- (iMO, $CD14^{pos}$ $CD16^{pos}$) monocytes accumulated in DLBCL peripheral blood and exhibited an inflammatory phenotype. On the opposite, nonclassical monocytes (ncMO, $CD14^{low}$ $CD16^{pos}$) were decreased in peripheral blood. Tumor-conditioned monocytes presented similarities with ncMO phenotype from DLBCL and were prone to migrate in response to CCL3, CCL5, and CXCL12, and presented similarities with DLBCL-infiltrated myeloid cells, as defined by mass cytometry. Finally, we demonstrated the adverse value of an accumulation of nonclassical monocytes in 2 independent cohorts of DLBCL.

Introduction

Circulating monocytes are classified by their CD14 and CD16 expression as classical- (cMO, $CD14^{pos}$ $CD16^{neg}$), intermediate- (iMO, $CD14^{pos}$ $CD16^{pos}$), and nonclassical- monocytes (ncMO, $CD14^{low}$ $CD16^{pos}$).[1] In addition, Slan expression (6-Sulfo LacNac, which is a carbohydrate modification of P-selectin glycoprotein ligand-1 [PSGL-1]), allows the sub-classification of ncMO $Slan^{pos}$ ($CD14^{low}$ $CD16^{pos}$ $Slan^{pos}$) and ncMO $Slan^{neg}$ ($CD14^{low}$ $CD16^{pos}$ $Slan^{neg}$).[2,3] Lastly monocytic myeloid derived suppressor cells (M-MDSC, $CD14^{pos}$ $HLA\text{-}DR^{low}$) found in acute or chronic inflammatory context, including cancers, are defined by an impairment of T- and NK-effector functions.[4] This nomenclature reflects pro-inflammatory, anti-inflammatory, or suppressive functions described for monocytes.[5,6]

In diffuse large B-cell lymphoma (DLBCL), tumor microenvironment (TME), myeloid cells are supportive of the neoplastic process.[7–10] In blood from DLBCL patients, an increase in circulating monocytes is a marker of adverse prognosis.[11–15]. However, so far monocytes were considered as a whole, and few studies analyzed the monocyte subsets and their clinical relevance even if their intrinsic functions are known to be different. Among monocyte subsets: i) $Slan^{pos}$ monocytes were increased and displayed high rituximab mediated antibody-dependent cellular cytotoxicity;[16] ii) an increase in $CD16^{pos}$ or $CD11b^{pos}CX3CR1^{pos}$ monocytes predicted poor progression free- and overall- survival;[17,18] iii) $CD14^{pos}CD163^{pos}PD\text{-}L1^{pos}$ monocytes were increased;[19] and finally iv) functional M-MDSCs were enriched in peripheral blood and predicted poor event-free survival.[20–22] In DLBCL tumor, the myeloid compartment heterogeneity was recently approached by high dimensional analysis revealing distinct macrophage phenotype across lymphoma subtypes.[23]

In light with the observation that various monocyte subsets are involved in the biology of DLBCL, we investigated the canonical cMO, iMO, ncMO Slan^{pos}, and ncMO Slan^{neg} subsets in two large cohorts of patients. We quantified these subsets, analyzed their phenotype and functions as well as the clinical relevance of these cells. We found here that in DLBCL, ncMO are prone to migrate into tissues and that their increase in peripheral blood is associated with an adverse prognosis.

Methods

Samples

A cohort of 91 DLBCL patients at diagnosis from the BMS-LyTRANS clinical trial (ClinicalTrials.gov Identifier: NCT01287923) was used in this study. Clinical characteristics of DLBCL patients enrolled in this training cohort are listed in Table 1. Patients with previous corticosteroid treatment were excluded from this study. As controls, age-matched heathy donors (HD, n = 49), follicular lymphomas (n = 9), mantle cell lymphomas (n = 9), chronic lymphocytic leukemias (n = 11), and marginal zone lymphomas (n = 10) were included. Part of these samples (DLBCL and HD) were used in a previous work.[22] Prognosis scores were validated in a second cohort of 155 DLBCL patients from the recently published GAINED trial (ClinicalTrials.gov Identifier: NCT01659099).[24] Clinical characteristics of DLBCL patients enrolled in this validation cohort are listed in Table 1. Finally, we reanalyzed CyTOF data (Flow Repository FR-FCM-Z2CA, already published by our group)[23] from myeloid cells from DLBCL tumors (n = 7). The research protocol was conducted under French legal guidelines and fulfilled the requirements of the local institutional ethics committee.

Fluorescent flow cytometry analysis

Blood samples were collected on heparin tubes. Flow cytometry analysis of M-MDSCs, cMO, iMO, and ncMO were performed on whole blood (300 µL/tube) with the antibody panel shown Table S1 and the gating strategy defined Figure S1. Absolute counts were obtained by using Flow-Count beads (Beckman Coulter, Brea, CA). An erythrocytes lysis (Uti-Lyse Dako, Carpinteria, CA) was performed before analysis by flow cytometry (Navios, Beckman Coulter). Analyses were performed using Kaluza software (Beckman Coulter).

In vitro culture

Monocytes were obtained from PBMCs by elutriation before cryopreservation (plate-forme DTC; CIC Biotherapie, Nantes, France). Monocytes were thawed and resuspended at 4 x10^6 cells/mL in RPMI 1640 (Invitrogen, Carlsband, CA, USA) supplemented with 10 % FCS and antibiotics (Invitrogen) and then diluted at 2 x10^6 cells/mL by adding, as control, the OCI-Ly medium (IMDM supplemented with 10% human AB serum,1% penicillin–streptomycin and 50 µM of β-Mercaptoethanol, or OCI-Ly3 or OCI-Ly19 supernatant. Two mL of cell suspension were seeded in a 6-well plate during 4 days before mass cytometry analysis or migration assay.

Mass cytometry analysis

Cell labeling and mass-cytometry analysis were performed as previously described.[25–27] Briefly, cells were incubated with 25 µM cisplatin (Fluidigm San Francisco, CA, USA). Then, 5 x10^6 cells were washed in PBS (HyClone Laboratories, Logan, UT, USA) containing 1 % BSA (Thermo Fisher Scientific) and stained in 100 µL PBS and BSA 1 %-containing Antibody cocktail. Cells were stained for 30 min at RT with the antibodies (Table S2) Cells were washed twice in PBS - BSA 1 % before

fixation in 1.6 % PFA, and permeabilization with methanol (Electron Microscopy Sciences, Hatfield, PA, USA). After incubating overnight at -20°C in MeOH, cells were washed twice with PBS -BSA 1 % and stained 20 min with iridium intercalator (Fluidigm, Sunnyvale, CA, US). Finally, cells were washed twice with PBS and twice with diH2O before acquisition a CyTOF 2.0 mass cytometer (Fluidigm).

Data processing and analysis

Data analysis was performed using the workflow previously developed.[23] Briefly, after acquisition, intrafile signal drift was normalized and .fcs files were obtained using CyTOF software. To diminish batch effects, all files were normalized on EQ Beads (Fluidigm) using the premessa R package (https://github.com/ParkerICI/premessa). Raw median intensity values were transformed to a hyperbolic arcsine (arcsinh) scale with a cofactor of 5, then analysis was performed using Cytobank software (Beckman Coulter, Brea, CA, USA). Each file was pre-gated for single, viable cells. These populations were exported as separate flow cytometry standard files and analyzed using Cyclospore.[28,29] The HSNE (Hierarchical Stochastic Neighbor Embedding) was performed to identify cell types. Then, hierarchical clustering of mean marker intensity on each cluster representing a phenotypically distinct myeloid cell population was performed.

Migration assay

At day 4 of monocyte culture with OCI-Ly3, or OCI-Ly19 supernatant, or control culture medium, cells were collected and washed twice in PBS before starvation during 1 hour (37°C) at 10^6 cells/mL in RPMI 1% HSA. Cells were washed once and 100 µL of cells at 10^6 cells/mL were added to the upper compartment of

Transwell chambers with 5 µM pore filters. The lower chamber contained CCL2 (R&D Systems, 30 ng/ml), CCL3 (R&D Systems, 20 ng/ml), CCL5 (R&D Systems, 30 ng/ml), CCL22 (R&D Systems, 20 ng/ml), CXCL5 (R&D Systems, 20 ng/ml), CXCL12 (R&D Systems, 20 ng/ml), or RPMI 1640 1% HSA as control. Cells in the lower chamber were collected after 5h and the absolute number of viable (DAPI negative) monocytes was quantified by flow cytometry using FlowCount beads.

Cell sorting

cMO ($CD19^{neg}$ $CD3^{neg}$ $CD335^{neg}$ $CD45^{pos}$ $CD14^{high}$ $CD16^{neg}$), iMO ($CD19^{neg}$ $CD3^{neg}$ $CD335^{neg}$ $CD45^{pos}$ $CD14^{high}$ $CD16^{pos}$), ncMO $Slan^{pos}$ ($CD19^{neg}$ $CD3^{neg}$ $CD335^{neg}$ $CD45^{pos}$ $CD14^{low}$ $CD16^{pos}$ $Slan^{pos}$), and ncMO $Slan^{neg}$ ($CD19^{neg}$ $CD3^{neg}$ $CD335^{neg}$ $CD45^{pos}$ $CD14^{low}$ $CD16^{pos}$ $Slan^{neg}$) were sorted from thawed PBMC of DLBCL patients and HD using an ARIA II (FACSAria, BD Biosciences).

Quantitative real-time PCR

Total RNA was extracted usingNucleospin® RNA XS kit (Macherey-Nagel, Duren, Germany). cDNA was then generated using Fluidigm Reverse Transcription Master Mix (Fluidigm). The qPCR were performed in triplicate using 96.96 Dynamic Array™ IFCs and the BioMark™ HD System from Fluidigm. For each sample, the mean CT value for the gene of interest was calculated, normalized to the geometric mean value of the 2 housekeeping genes (*CDKN1B,* and *ELF1*) (Table S3), and compared to the median value obtained from the reference population (HD cMO or iMO for Figure 2, and DLBCL ncMO for Figure 3) using the 2-ddCT method. Results were expressed as the ratio of sample mean to reference mean for each gene.

192 **Statistical analysis**

193 Statistical analyses were performed with GraphPad Prism 8.4.3 software
194 (GraphPad Software, San Diego, CA, USA) using Spearman correlation, Wilcoxon,
195 Mann-Whitney, Ordinary one-way ANOVA with Tukey's multiple comparisons test,
196 and Fishers's exact tests as appropriate. Optimal thresholds were defined with the
197 *maxstat* package, log-rank tests were performed with the *survminer* package, cox
198 model for univariate and multivariate analysis were performed with the *survival*
199 package. Analyses were generated with R v4.0.3, using Rstudio v1.3.1093.

200

201 **Data sharing statement**

202 For original data, please contact the corresponding author.

203

204 **Results**

205 **cMO and iMO are increased in DLBCL**

206 We have previously shown that M-MDSCs accumulated in DLBCL peripheral
207 blood.[22] However, this increase accounts for only a part of the total monocyte
208 accumulation suggesting that additional monocyte subsets are also increased in
209 DLBCL samples (Figure 1A). We quantified the absolute count of the 4 circulating
210 monocyte subsets M-MDSC, cMO, iMO, and ncMO. M-MDSC, cMO, and iMO were
211 increased in DLBCL when compared to HDs ($P < .05$, median: 5.75 $x10^6$ cells/L vs
212 2.8 $x10^6$ cells/L, 348.8 $x10^6$ cells/L vs 274.1 $x10^6$ cells/L, and 34.4 $x10^6$ cells/L vs
213 26.1 $x10^6$ cells/L; respectively). Conversely, ncMO were significantly decreased in
214 DLBCL when compared to HD ($P < .0001$, median: 17.1 $x10^6$ cells/L vs 36.1 $x10^6$
215 cells/L; Figure 1B). Noteworthy, whereas the increase of cMO and iMO was also
216 found in other B cell lymphomas, this decrease in ncMO was specific of DLBCL

(Figure S2). Then, we wondered in which monocyte subset M-MDSCs were included. Of note M-MDSC count was correlated with total monocyte (R = .70, P < .0001), cMO (R = .55, P < .0001), and iMO (R = .74, P < .0001) but was not correlated with ncMO (Figure 1C) No correlation were observed between MO subsets in HD samples (data not shown). Regarding CD14 and CD16 expression, M-MDSCs were essentially aligned with the cMO phenotype and to a lesser extent to iMO (Figure 1D). Altogether, these results confirmed that in addition to MDSCs, cMO and iMO were also involved in the monocyte increase observed in DLBCL patients.

DLBCL cMO and iMO share a common inflammatory phenotype

To further identify the immune properties of monocyte subsets, we sorted cMO and iMO from DLBCL (n=7) and HD (n=4) samples. Gene expression was assessed by high throughput qPCR on 71 genes involved in myeloid biology[22] (Table S3 and Figure S3). Of note, 6 cMO and 5 iMO out of 7 DLBCL were clustered (Figure 2A and Figure S3). DLBCL cMO and DLBCL iMO were significantly enriched for *FCGR3A, CD36, FCGR1A, CYBB, AIM2, STAT6, FCGR2A, CCR2, NLRC4, S100A8,* and *CD14* genes, when compared to the corresponding subsets in HDs (P <.05, |log2FC|>1) (Figure 2B). In addition, *S100A9* and *CD163* were also increased in DLBCL cMO, whereas *CD33* and *ITGAM* were enriched only in DLBCL iMO. For both subsets, *SLC7A11*, *CD274*, and *CXCL1* were expressed at lower levels in DLBCLs (Figure 2B). Biological processes enriched in DLBCL cMO and iMO included apoptosis, production of ROS, immune response, and phagocytosis (Figure 2C). By flow cytometry, we showed that cMO and iMO from DLBCL displayed a higher expression of CD64 and CCR2 (P < .05), without variation in HLA-DR and CD163

(Figure 2D). Altogether, these results suggested that, in DLBCL, cMO and iMO share a common deregulated inflammatory phenotype.

DLBCL ncMO are decreased in peripheral blood and exhibit an inflammatory- and tolerogenic- phenotype

We then focused on ncMO in DLBCL samples and found that both subsets of ncMO (ncMO Slan^{pos} and ncMO Slan^{neg}) were decreased in DLBCLs when compared to HDs (ncMO Slan^{pos} median at 3.3 x10^6 cells/L vs 9.1 x10^6 cells/L [$P < .001$] and ncMO Slan^{neg} median at 19 x10^6 cells/L vs 23.7 x10^6 cells/L [$P < .05$], respectively) (Figure 3A). No increase of apoptosis was detected in ncMO from DLBCL patients (data not shown). Then, sorted ncMO Slan^{pos} and ncMO Slan^{neg} from DLBCL and HD samples were analyzed by high-throughput Q-PCR (Figure S4). To explore the similarities between ncMO Slan^{pos}, ncMO Slan^{neg}, iMO, and cMO, we performed a hierarchical clustering on the DLBCL samples. For 6 out of 7 patients, cMO and iMO were separated from ncMO independently of Slan expression (Figure 3B and Figure S5). In addition, ncMO exhibited tolerogenic genes (*PDCD1LG2, IL10, IDO, CD274, AGER, TNFAIP6*) (Figure S5), most of these genes were not expressed in HD ncMO (Figure S6). In DLBCL, cMO and iMO in one hand and ncMO Slan^{pos} and ncMO Slan^{neg} in the other hand shared similar gene expression (Figure 2A and Figure S5), thus we compared the gene expression between ncMO, irrespectively of the Slan status, and both cMO and iMO. DLBCL ncMO were enriched for both inflammatory (*CXCL10, AIM2, IL12A*) and tolerogenic (*PDCD1LG2, IL10, IDO, CD274, AGER*) genes ($P < .05$, $|log2FC| > 1$) compared to cMO and iMO (Figure 3C). Biological processes involved by genes enriched in ncMO from DLBCL patients were growth of tumor, inhibition of cells, and chemotaxis (Figure 3D and Figure S7).

Tumor conditioned monocytes give rise to ncMO-like prone to migrate in response to CCL3, CCL5, and CXCL12

In order to evaluate how tumor B cells contribute directly to the phenotype of DLBCL monocytes, we cultured monocytes from HD with supernatants from the DLBCL cell lines OCI-Ly3 and OCI-Ly19. After coculture, we analyzed the monocyte phenotype by mass cytometry.[23,25] After dimension reduction and clustering (Figure 4A), we noticed an increased expression of Slan, CD64, CD163, CD86, CD206, and CD16 and a decreased expression of CCR2 in clusters from tumor-conditioned monocytes when compared to non-conditioned counterparts. We concluded that tumor conditioned monocytes acquired a ncMO-like phenotype. Then we wondered if these cells were prone to migrate into tissue. Tumor-conditioned monocytes demonstrated an increase in *in vitro* migration in response to CCL3 (46.4 and 18.2 fold for OCI-Ly3 and OCI-Ly19, respectively), CCL5 (78.4 and 63.4 fold for OCI-Ly3 and OCI-Ly19, respectively), and CxCL12 (131 and 77.4 fold for OCI-Ly3 and OCI-Ly19, respectively), when compared to non-conditioned monocytes (Figure 4B). Then we compared the phenotype obtained by mass cytometry of tumor-conditioned monocytes (Mo OCI-Ly) to the phenotype of myeloid cells from DLBCL tumors, already published by our group (Flow Repository FR-FCM-Z2CA).[23] Interestingly, a subset of myeloid cells from DLBCL showed similarities with tumor-conditioned monocytes, in particular with the common high expression of CD64, CD11c, CD32, S100A9, and HLA-DR (Figure 4C).

High level of circulating ncMO is correlated with an adverse prognosis in DLBCL

Then, we evaluated the prognosis value of cMO, iMO, and ncMO in DLBCL. We used i) the proportion of ncMO to other monocytes (ratio ncMO to sum of cMO and iMO) and ii) the absolute count of circulating cMO, iMO, and ncMO. Analysis was performed on 52 patients for which clinical data were available. cMO and iMO were not associated with prognosis (data not shown). By contrast, patients with high proportion of ncMO and high absolute count of circulating ncMO were associated with a lower event-free survival probability (P = .043 and P = .0061, respectively) using thresholds (ratio at 0.06 and ncMO at 20.58 $x10^6$ cells/L) defined with the maxstat package (Figure 5A, Figure S8A and Figure S8B).

To validate the prognosis value of ncMO obtained on this training cohort, we analyzed by flow cytometry the proportion of monocyte subsets in an independent cohort of 155 DLBCL samples from the recently published GAINED trial (NCT01659099).[24] With the previously calculated thresholds, high proportion of ncMO and high absolute count of ncMO was associated with a lower overall survival (P = .017 and P = .011, respectively) (Figure 5A and Figure S8B). A univariate analysis on the validation cohort showed that Ann Arbor Stage III-IV, ECOG status >1, elevated LDH, PET4 positivity, and increase in circulating ncMO were associated with lower OS (Table S4). In a multivariable analysis Ann Arbor Stage III-IV, PET4 positivity, increase in circulating ncMO remained statistically significant (Table S4).

We previously demonstrated the accumulation of M-MDSC in DLBCL[22] and since no phenotypic overlap existed between M-MDSC and ncMO (Figure 1D), we wondered if patients' characteristics were different between M-MDSC^{high} and ncMO^{high} DLBCLs. Both M-MDSC and ncMO were infrequently increased together (11 cases out of 155 [7.1 %]); ncMO were increased alone in 51 cases (32.9 %), and M-MDSC were increased alone in 28 cases (18.1 %) (Figure 5B). Interestingly,

316 ncMO^{high} and M-MDSC^{high} patients corresponded to different types of patients. In
317 particular when compared to ncMO^{low}, ncMO^{high} were enriched in ABC DLBCL
318 subtypes (37.5 *vs* 15.9 % [P = .014]) and in older patients (median age at 50 *vs* 46
319 years [P = .044]). On the other hand, when compared to ncMO^{high}, M-MDSC^{high}
320 patients were younger (median age at 42 *vs* 50 years [P = .0027]) and had higher
321 levels of soluble PD-L1 (sPD-L1 at 1849 *vs* 1142 pg/mL [P = .008]) (Figure 5B).
322
323 **Discussion**
324 Although the prognostic relevance of total monocyte count has been described
325 in large cohorts of DLBCL in the last decade,[11–15] few studies evaluated which
326 particular monocyte subset was involved. In a previous work, we have shown an
327 accumulation of M-MDSC (CD14^{pos} HLA-DR^{low}) in peripheral blood from DLBCL
328 patients.[22] Because M-MDSCs were not responsible for the whole increase in
329 monocytes in our cohort, we explored cMO, iMO, and ncMO subsets. We
330 demonstrated an increase in cMOs and iMOs in DLBCL, as in other lymphomas
331 subtypes tested (CLL, MCL, MZL, and FL). In DLBCL, these MO subsets shared an
332 inflammatory phenotype. By contrast, ncMOs were decreased in peripheral blood
333 only in DLBCLs when compared to HDs or other B cell lymphomas. Interestingly,
334 high number of circulating ncMO was an adverse prognosis in 2 independent cohorts
335 of DLBCL patients. Finally, we found that tumor-conditioned monocytes shared a
336 common phenotype with ncMOs and were prone to migrate in response to
337 chemokines.
338 Surprisingly cMO and iMO from DLBCL shown common deregulated pathways
339 with an enrichment for *FCGR3A, CD36, FCGR1A, CYBB, AIM2, STAT6, FCGR2A,*
340 *CCR2, NLRC4, S100A8,* and *CD14*. These genes are broadly expressed in cMO in

341 healthy samples[2,5] and our results suggest that iMO and cMO are tumor-educated
342 and polarized to a common inflammatory phenotype in DLBCL. In our study we found
343 a decrease in both circulating ncMO Slan^{neg} and ncMO Slan^{pos} when compared to
344 HDs, whereas an increase in ncMO Slan^{pos} was previously described in DLBCL.[16]
345 This discrepancy might be explained by differences in patient characteristics between
346 both studies. In particular patients were older in the study from Verni et coll (63.9
347 years [range: 31-86] *vs* 50 years [range:18-83]) and at higher grade (clinical stage III-
348 IV at 80.5% *vs* 70% and IPI ≥3 at 55.6% *vs* 40%).[16] In CLL, an increase of ncMO
349 correlates with high cytogenetic risk (deletion 11q, 17p, or trisomy 12).[30] In our study,
350 an increase of the proportion of circulating ncMO was a worse prognosis factor in 2
351 independent cohorts. This was previously suggested on 45 DLBCLs where the
352 decrease of CD16^{pos} monocyte to CD16^{neg} monocyte ratio predicted poor prognosis,
353 however conclusions were limited because iMO and cMO were analyzed conjointly.[17]
354 ncMO abundance also predicted patient survival of pediatric and adult B acute
355 lymphoblastic leukemia.[31] Interestingly, in a pre-clinical mouse model of B cell
356 lymphomas, Ly6C^{low} monocytes (corresponding to the ncMO)[32] accumulated and
357 showed high levels of immunosuppressive genes (*PD-L1, PD-L2, Arg1, IDO1, and*
358 *CD163*) associated with suppression of T cell proliferation.[33] In colorectal cancer
359 Ly6C^{low} monocyte mediated immunosuppression by IL-10 production.[34] Finally, ncMO
360 were increased in gastric cancer.[35] Conversely, in a lung cancer model, LyC^{low}
361 monocytes recruited NK cells to prevent cancer metastasis.[36] In DLBCL, we and
362 others focused on total monocyte and on M-MDSC and few attention was given to
363 other monocyte subsets. Interestingly, ncMO and M-MDSC have non-overlapping
364 phenotype regarding HLA-DR expression and these cells infrequently correlated in
365 patients suggesting different mechanism of myelopoiesis dysregulation. Patients that

were enriched in circulating MDSCs were younger and presented high amount of sPD-L1, a pejorative marker.[37] Interestingly, release of PD-L1 was a mechanism of immune suppression suggested in DLBCL.[22]

Beside immunosuppression, gene enriched in ncMO were related to chemotaxis. Circulating ncMO are diminished in DLBCL, on the contrary there were enriched in other B cell lymphomas or solid tumor,[38] thus we hypothesized that these cells might migrate into tissue to contribute to the tumor-associated macrophage compartment. CCL2, CCL3, CCL5, CCL22, CXCL5, and CXCL12 are involved in monocyte, MDSC, and macrophage recruitment into the TME.[39] Tumor-conditioned monocyte shown an increased migration in response to CXCL5, CXCL12, CCL3, and CCL5. Consistently, in our previous study, *CXCL5* expression was increased in peripheral blood from DLBCL compared to healthy donors and its expression was related to a worse event-free survival.[22] CCL3 is also increased in DLBCL when compared to HD and high level correlates with shorter survival.[40,41]

In DLBCL, TAM are heterogenous,[23] in particular a Slan^{pos} macrophage subset is involved in rituximab mediated antibody dependent cellular cytotoxicity.[16] In agreement, we found in DLBCL a compartment of cells expressing Slan at high level with CD14, CD32, and HLA-DR. However, DLBCL clusters that correlated with tumor-conditioned monocytes highly expressed CD64, CD36, and S100A9 and thus presented similarities with IFNγ *in-vitro* polarized macrophages.[25] Few studies compared paired samples from circulating and in situ myeloid cells. In melanoma patient, myeloid cells obtained from the blood, but not from the tumor, were suppressive.[42] In lung adenocarcinoma, macrophages phenotype detected in tumor were not present in peripheral blood.[43] Currently, there is no model of lymphoma that allows tracking the myeloid cell from the blood to the tissues. Future studies entailing

391 a prospective collection of paired blood and tumor samples are needed to confirm
392 these observations on ncMO and to put in perspective the myeloid compartment with
393 the T/NK compartment. Also, it would be interested to test the prognosis value in
394 cohort of DLBCL treated with other immunotherapies and correlate with responders
395 vs non-responders.

396 Our study as some limitations, in particular the lack of extensive functional
397 studies due to the low number of circulating ncMO in DLBCL samples precluding
398 large cell sorting. Taken together, our results show that ncMO are involved in the
399 DLBCL physiopathology and impact the prognosis of the disease. Given the current
400 and our previous data, we propose that cMO and iMO are reflecting the inflammatory
401 status in DLBCL, whereas M-MDSC are responsible of a systemic suppressive
402 response, and ncMO are involved in suppressive response and migration to tissue.
403

Acknowledgements

This work was supported by a fellowship from the Nuovo-Soldati Foundation (Switzerland) (M.R.), from the Ligue contre le Cancer (M.R.), from the COmite de la REcherche Clinique et Translationnelle, CHU of Rennes (F.L.), from the Association pour le Développement de l'Hématologie Oncologie (F.L.), from the National Institute of Cancer (INCa Recherche Translationnelle 2010) (T.F.), and from the Groupe Ouest-Est des Leucémies et des Autres Maladies du Sang (GOELAMS) (T.F.). We are indebted to the clinicians of the BREHAT network and to the French Blood Bank (EFS) of Rennes for providing samples. The authors acknowledge the Centre de Ressources Biologiques (CRB-santé) of Rennes (BB-0033-00056) for managing samples.

Authorship contributions

S.L.Ga., F.L., A.M., C.M., and I.A. designed and performed experiments, analyzed data; J.M.I., D.R., J.F., and T.J.M. analyzed data; C.P., K.B., G.D., G.C., P.G., S.L.Go., R.O.C., R.H., and T.L. provided samples; T.F. and K.T. raised the funds and analyzed data; M.R. designed and supervised research, analyzed data, and wrote the paper. All authors revised the manuscript.

Disclosure of conflicts of interest

All authors declare no conflicts of interest.

References

1. Ziegler-Heitbrock L, Ancuta P, Crowe S, et al. Nomenclature of monocytes and dendritic cells in blood. *Blood*. 2010;116(16):e74-80.

2. Cros J, Cagnard N, Woollard K, et al. Human CD14dim Monocytes Patrol and Sense Nucleic Acids and Viruses via TLR7 and TLR8 Receptors. *Immunity*. 2010;33(3):375–386.

3. Ahmad F, Döbel T, Schmitz M, Schäkel K. Current Concepts on 6-sulfo LacNAc Expressing Monocytes (slanMo). *Front Immunol*. 2019;10:948.

4. Bronte V, Brandau S, Chen S, et al. Recommendations for myeloid-derived suppressor cell nomenclature and characterization standards. *Nature Communications*. 2016;7:12150.

5. Wong KL, Tai JJ-Y, Wong W-C, et al. Gene expression profiling reveals the defining features of the classical, intermediate, and nonclassical human monocyte subsets. *Blood*. 2011;118(5):e16-31.

6. Guilliams M, Mildner A, Yona S. Developmental and Functional Heterogeneity of Monocytes. *Immunity*. 2018;49(4):595–613.

7. Lenz G, Wright G, Dave SS, et al. Stromal gene signatures in large-B-cell lymphomas. *The New England journal of medicine*. 2008;359(22):2313–2323.

8. Riihijarvi S, Fiskvik I, Taskinen M, et al. Prognostic influence of macrophages in patients with diffuse large B-cell lymphoma: a correlative study from a Nordic phase II trial. *Haematologica*. 2015;100(2):238–245.

9. Scott DW, Gascoyne RD. The tumour microenvironment in B cell lymphomas. *Nature Reviews Cancer*. 2014;14(8):517–534.

10. Nam SJ, Kim S, Kwon D, et al. Prognostic implications of tumor-infiltrating macrophages, M2 macrophages, regulatory T-cells, and indoleamine 2,3-dioxygenase-positive cells in primary diffuse large B-cell lymphoma of the central nervous system. *Oncoimmunology*. 2018;7(7):1–39.

11. Tadmor T, Bari A, Sacchi S, et al. Monocyte count at diagnosis is a prognostic parameter in diffuse large B-cell lymphoma: results from a large multicenter study involving 1191 patients in the pre- and post-rituximab era. *Haematologica*. 2014;99(1):125–130.

12. Nitta H, Terui Y, Yokoyama M, et al. Absolute peripheral monocyte count at diagnosis predicts central nervous system relapse in diffuse large B-cell lymphoma. *Haematologica*. 2015;100(1):87–90.

13. Troppan K, Deutsch A, Gerger A, et al. The derived neutrophil to lymphocyte ratio is an independent prognostic factor in patients with diffuse large B-cell lymphoma. *British Journal of Cancer*. 2014;110(2):369–374.

14. Wilcox RA, Ristow K, Habermann TM, et al. The absolute monocyte and lymphocyte prognostic score predicts survival and identifies high-risk patients in diffuse large-B-cell lymphoma. *Leukemia*. 2011;25(9):1502–1509.

15. Maurer MJ, Jais J-P, Ghesquières H, et al. Personalized risk prediction for event-free survival at 24 months in patients with diffuse large B-cell lymphoma. *American journal of hematology*. 2016;91(2):179–184.

16. Vermi W, Micheletti A, Finotti G, et al. slan+ Monocytes and Macrophages Mediate CD20-Dependent B-cell Lymphoma Elimination via ADCC and ADCP. *Cancer Research*. 2018;78(13):3544–3559.

17. Han X, Ruan J, Zhang W, et al. Prognostic implication of leucocyte subpopulations in diffuse large B-cell lymphoma. *Oncotarget*. 2017;8(29):47790–47800.

18. Yhim H-Y, Kim J-A, Ko S-H, et al. The prognostic significance of CD11b+CX3CR1+ monocytes in patients with newly diagnosed diffuse large B-cell lymphoma. *Oncotarget*. 2017;8(54):92289–92299.

19. Vari F, Arpon D, Keane C, et al. Immune evasion via PD-1/PD-L1 on NK cells and monocyte/macrophages is more prominent in Hodgkin lymphoma than DLBCL. *Blood*. 2018;131(16):1809–1819.

20. Lin Y, Gustafson MP, Bulur PA, et al. Immunosuppressive CD14+HLA-DRlow/- monocytes in B-cell non-Hodgkin lymphoma. *Blood*. 2011;117(3):872–881.

21. Xiu B, Lin Y, Grote DM, et al. IL-10 induces the development of immunosuppressive CD14(+)HLA-DR(low/-) monocytes in B-cell non-Hodgkin lymphoma. *Blood Cancer Journal*. 2015;5(7):e328.

22. Azzaoui I, Uhel F, Rossille D, et al. T-cell defect in diffuse large B-cell lymphomas involves expansion of myeloid-derived suppressor cells. *Blood*. 2016;128(8):1081–1092.

23. Roussel M, Lhomme F, Roe CE, et al. Mass cytometry defines distinct immune profile in germinal center B-cell lymphomas. *Cancer Immunology, Immunotherapy*. 2020;69(3):407–420.

24. Gouill SL, Ghesquieres H, Obéric L, et al. Obinutuzumab versus Rituximab in young patients with advanced DLBCL, a PET-guided and randomized phase 3 study by LYSA. *Blood*. 2020;1–35.

25. Roussel M, Ferrell PB, Greenplate AR, et al. Mass cytometry deep phenotyping of human mononuclear phagocytes and myeloid-derived suppressor cells from human blood and bone marrow. *Journal of Leukocyte Biology*. 2017;102(2):437–447.

26. Roussel M, Bartkowiak T, Irish JM. Picturing Polarized Myeloid Phagocytes and Regulatory Cells by Mass Cytometry. *Methods in molecular biology*. 2019;1989(2018):217–226.

496 27. Ferrant J, Lhomme F, Gallou SL, Irish JM, Roussel M. Circulating Myeloid Regulatory
497 Cells: Promising Biomarkers in B-Cell Lymphomas. *Front Immunol*. 2021;11:623993.

498 28. Höllt T, Pezzotti N, Unen V van, et al. Cytosplore: Interactive Immune Cell Phenotyping
499 for Large Single□Cell Datasets. *Comput Graph Forum*. 2016;35(3):171–180.

500 29. Unen V van, Höllt T, Pezzotti N, et al. Visual analysis of mass cytometry data by
501 hierarchical stochastic neighbour embedding reveals rare cell types. *Nat Commun*.
502 2017;8(1):1740.

503 30. Maffei R, Bulgarelli J, Fiorcari S, et al. The monocytic population in chronic lymphocytic
504 leukemia shows altered composition and deregulation of genes involved in phagocytosis and
505 inflammation. *Haematologica*. 2013;98(7):1115–1123.

506 31. Witkowski MT, Dolgalev I, Evensen NA, et al. Extensive Remodeling of the Immune
507 Microenvironment in B Cell Acute Lymphoblastic Leukemia. *Cancer cell*. 2020;37(6):867-
508 882.e12.

509 32. Ginhoux F, Jung S. Monocytes and macrophages: developmental pathways and tissue
510 homeostasis. *Nature Reviews Immunology*. 2014;14(6):392–404.

511 33. McKee SJ, Tuong ZK, Kobayashi T, et al. B cell lymphoma progression promotes the
512 accumulation of circulating Ly6Clo monocytes with immunosuppressive activity.
513 *Oncoimmunology*. 2018;7(2):e1393599.

514 34. Jung K, Heishi T, Khan OF, et al. Ly6Clo monocytes drive immunosuppression and
515 confer resistance to anti-VEGFR2 cancer therapy. *The Journal of clinical investigation*.
516 2017;127(8):3039–3051.

517 35. Eljaszewicz A, Jankowski M, Gackowska L, et al. Gastric cancer increase the percentage
518 of intermediate (CD14++CD16+) and nonclassical (CD14+CD16+) monocytes. *Clinical*
519 *Immunology*. 2012;4:355–361.

520 36. Hanna RN, Cekic C, Sag D, et al. Patrolling monocytes control tumor metastasis to the
521 lung. *Science*. 2015;350(6263):985–990.

522 37. Rossille D, Azzaoui I, Feldman AL, et al. Soluble programmed death-ligand 1 as a
523 prognostic biomarker for overall survival in patients with diffuse large B-cell lymphoma: a
524 replication study and combined analysis of 508 patients. *Leukemia*. 2017;31(4):988–991.

525 38. Cassetta L, Fragkogianni S, Sims AH, et al. Human Tumor-Associated Macrophage and
526 Monocyte Transcriptional Landscapes Reveal Cancer-Specific Reprogramming, Biomarkers,
527 and Therapeutic Targets. *Cancer Cell*. 2019;35(4):588-602.e10.

528 39. Nagarsheth N, Wicha MS, Zou W. Chemokines in the cancer microenvironment and their
529 relevance in cancer immunotherapy. *Nature Reviews Immunology*. 2017;17(9):559–572.

530 40. Charbonneau B, Maurer MJ, Ansell SM, et al. Pretreatment circulating serum cytokines
531 associated with follicular and diffuse large B-cell lymphoma: A clinic-based case-control
532 study. *Cytokine*. 2012;60(3):882–889.

533 41. Takahashi K, Sivina M, Hoellenriegel J, et al. CCL3 and CCL4 are biomarkers for B cell
534 receptor pathway activation and prognostic serum markers in diffuse large B cell lymphoma.
535 *Brit J Haematol*. 2015;171(5):726–735.

536 42. Gros A, Turcotte S, Wunderlich JR, et al. Myeloid Cells Obtained from the Blood but Not
537 from the Tumor Can Suppress T-cell Proliferation in Patients with Melanoma. *Clinical*
538 *Cancer Research*. 2012;18(19):5212–5223.

539 43. Lavin Y, Kobayashi S, Leader A, et al. Innate Immune Landscape in Early Lung
540 Adenocarcinoma by Paired Single-Cell Analyses. *Cell*. 2017;169(4):750-757.e15.

541

542

Table 1: Patient's characteristics at baseline

	Healthy donors (n = 49)	BMS-LyTRANS Training cohort (n = 91)	GAINED[24] Validation cohort (n=155)
Average age, years (range)	52.9 (25-66)	55.7 (18-83)	44.9 (19-60)
Male, n (%)	30 (61.2%)	56 (61.5%)	86 (55.5%)
Female, n (%)	19 (38.8%)	35 (38.5%)	69 (44.5%)
aaIPI, n (%)			
0 to 1	NA	46 (59%)*	68 (43.9%)
2	NA	28 (35.9%)*	71 (45.8%)
3	NA	4 (5.1%)*	16 (10.3%)
Cell of origin, n (%)			
GCB (Hans[&] or Nanostring[@])	NA	30 (54.5%)*,[&]	83 (74.8%)*,[@]
Non-GCB (Hans[&]) or ABC (Nanostring[@])	NA	25 (45.5%)*,[&]	28 (25.2%)*,[@]
Unclassified[@]	NA	NA	9[@]
Insufficient material	NA	36	35
Chemotherapy, n			
Rituximab CHOP	NA	69	37
Rituximab ACVBP	NA	0	39
Obinutuzumab CHOP	NA	6	40
Obinutuzumab ACVBP	NA	0	38
Other treatment	NA	3	0
Unknown or not treated	NA	13	1

aaIPI: age adjusted International prognostic index; GCB: germinal center B cell; ABC: activated B cell *: percentage among cases with known data; [&]: defined by Hans algorithm; [@]: defined by nanostring analysis. CHOP: cyclophosphamide, doxorubicine, vincristine, and prednisone; ACVBP: doxorubicine, prednisone, cyclophosphamide, vindesine, and bleomycine; NA: not applicable.

Figure Legends

Figure 1: cMO and iMO are increased in peripheral blood from DLBCL. (A) Monocyte absolute counts in HD (n = 43) and DLBCL (n = 69). For the 23 DLBCL samples with monocyte above 528 $x10^6$ monocytes/L (corresponding to the 90^{th} percentile of HD), proportion of M-MDSC within monocyte (B) M-MDSC in HD (n = 43) and DLBCL (n = 69) and monocyte subset counts (classical- [cMO], intermediate- [iMO], and nonclassical- [ncMO]) in peripheral blood from HD (n = 55) and DLBCL patients (n = 91). (C) Pearson correlation between M-MDSC and monocyte (MO), cMO, iMO, and ncMO (n = 69). (D)- Mean fluorescent intensity (MFI) for CD14, CD16, and HLA-DR. Each dot represents a DLBCL sample (n = 33) colored by monocyte subset (MDSC, cMO, iMO, and ncMO). *P < .05, **P < .01, ****P < .0001.

Figure 2: Circulating cMO and iMO share a common inflammatory phenotype, in DLBCL. (A) Hierarchical clustering of classical- (cMO) and intermediate- (iMO) monocytes, from HD (n = 4) and DLBCL (n = 7) samples. See Table S3 for a list of genes analyzed on monocyte subsets after cell sorting. Pearson's correlation and complete linkage was employed. (B) Transcripts differentially expressed (P < .05; |log2FC| > 1) between DLBCLs and HDs, for cMO and iMO. (C) Predicted top 5 biological processes increased for cMO and iMO from DLBCL (Ingenuity Pathway Analysis, z-score > 2.5, ranked by p-value). (D) Mean fluorescence (MFI) for CD64, HLA-DR, CD163, CD14, CD16, and CCR2 for HD (n = 16) and DLBCL (n = 33) samples. **P < .01, ***P < .001, ns: non significant.

Figure 3: ncMO are decreased in peripheral blood but exhibit an inflammatory- and tolerogenic- phenotype. (A) Nonclassical $Slan^{pos}$ or $Slan^{neg}$ ($ncMOSlan^{pos}$ and $ncMoSlan^{neg}$) monocytes from HDs (n = 28) and DLBCLs (n = 56). (B) Hierarchical clustering of classical- (cMO), intermediate- (iMO), nonclassical $Slan^{pos}$- or $Slan^{neg}$- ($ncMOSlan^{pos}$ and $ncMoSlan^{neg}$) monocytes from DLBCL (n = 7) samples. DLBCL identity (#). List of genes analyzed on monocyte subsets after cell sorting is on Table S3. Pearson's correlation and complete linkage was employed. (C) Transcripts (P < .05; |log2FC| > 1) enriched in ncMO compared to cMO and iMO for DLBCL. (D) Predicted top 5 biological processes increased for ncMO compared to cMO and iMO, from DLBCL (Ingenuity Pathway Analysis, z-score > 2.5, ranked by p-value).

Figure 4: Tumor cells supernatants polarize monocytes with higher migratory abilities. (A) Monocytes from healthy donors were treated with OCI-Ly supernatant (n = 2) or vehicle as control (n = 2). After CyTOF analysis, myeloid cells (12,000 to 30,000) were clustered (n = 33 clusters). Mean marker intensities are shown on a heatmap for each cluster (left). Selected markers are shown for monocytes treated or not with OCI-Ly supernatant (right). (B) Migration assay for HD monocytes cultured or not with OCI-Ly3 and OCI-Ly19 supernatant in response to CCL2, CCL3, CCL5, CCL22, CXCL5, and CXCL12. (C) Phenotype comparison of tumor conditioned monocytes and myeloid cells from DLBCL tumors (n = 7) (FR-FCM-Z2CA, already published by our group).[22] Mean marker intensities are shown on a heatmap for each cluster. The abundance of clusters is shown as well as the enrichment in tumor-conditioned monocytes (Mo OCI-Ly) and in myeloid cells from DLBCL tumors (DLBCL).

Figure 5: High levels of circulating ncMO is correlated to adverse prognosis in DLBCL. (A) Event-free survival (EFS) in training cohorts (NCT01287923) and overall survival (OS) in validation cohorts (NCT01659099).[24] Patients were stratified on the ratio of ncMO to other monocytes (cMO and iMO). Threshold was defined on the training cohort using the maxstat package (Figure S8). Survival probability was calculated for both groups with a log-rank test. (B) Absolute count for ncMO (threshold at 20.58 $x10^6$ cells/L) and M-MDSC (threshold at 22.51 $x10^6$ cells/L)[22] and distribution of age and soluble PD-L1 (sPD-L1), *P < .05, **P < .01.

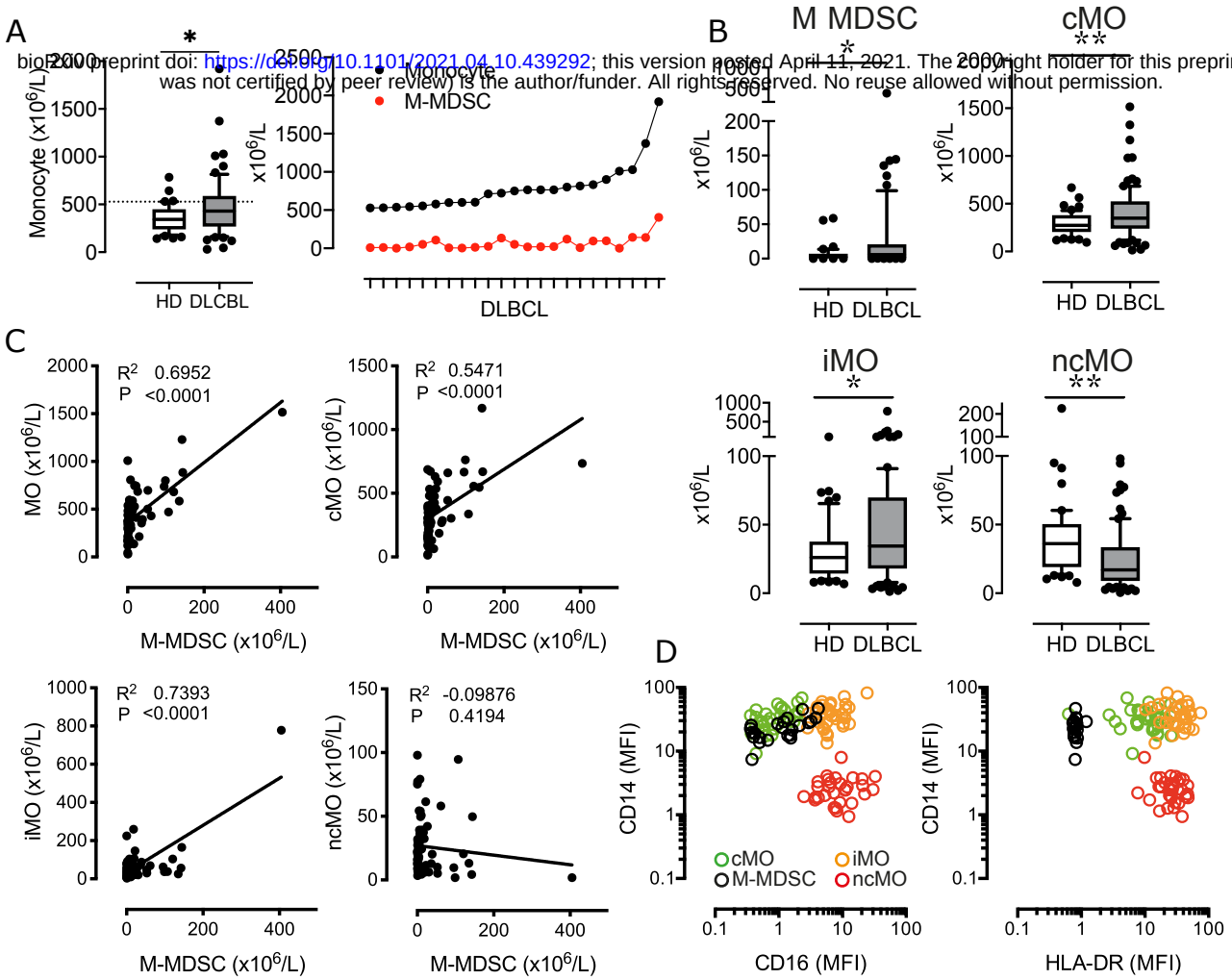

Figure 1

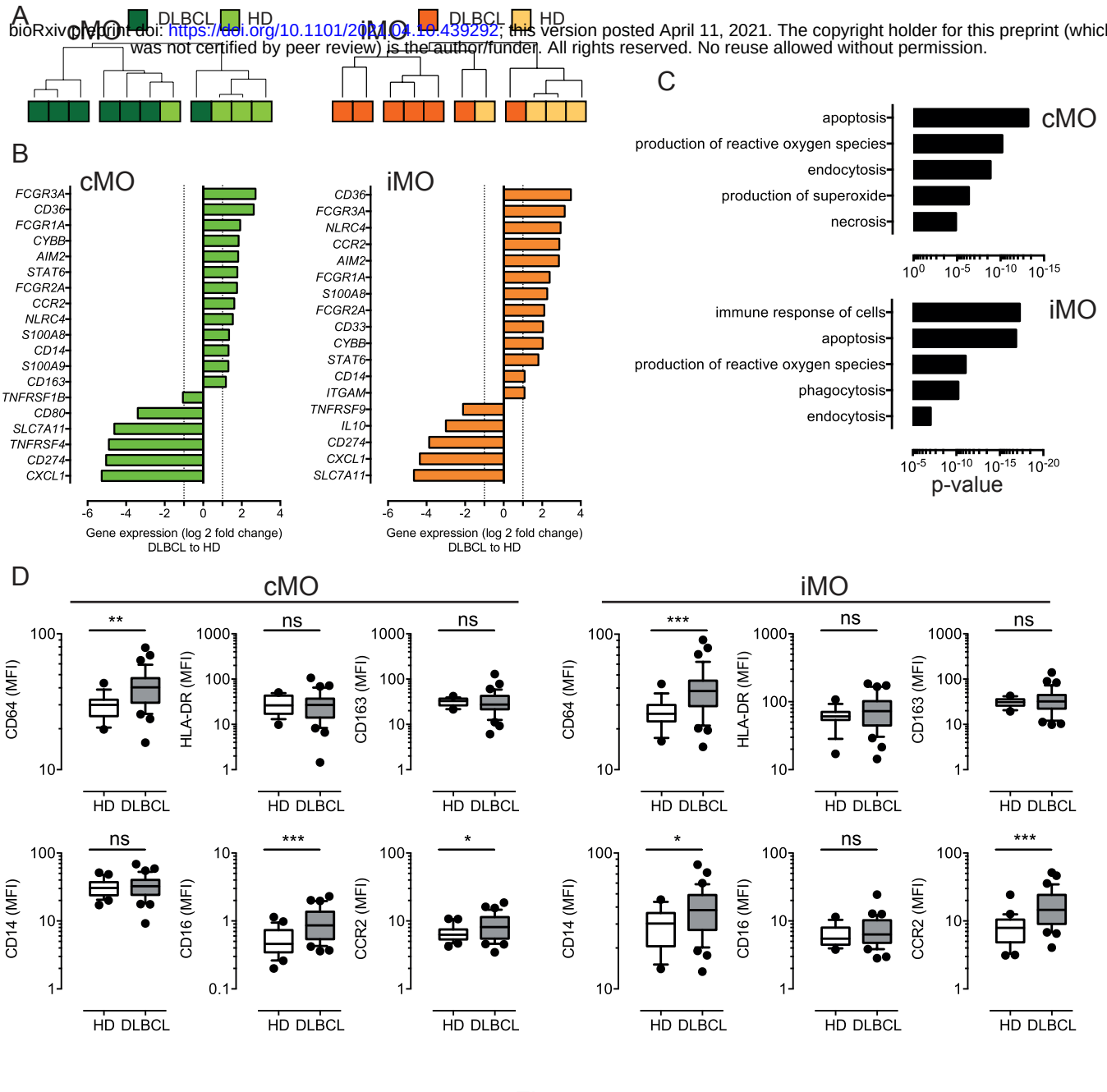

Figure 2

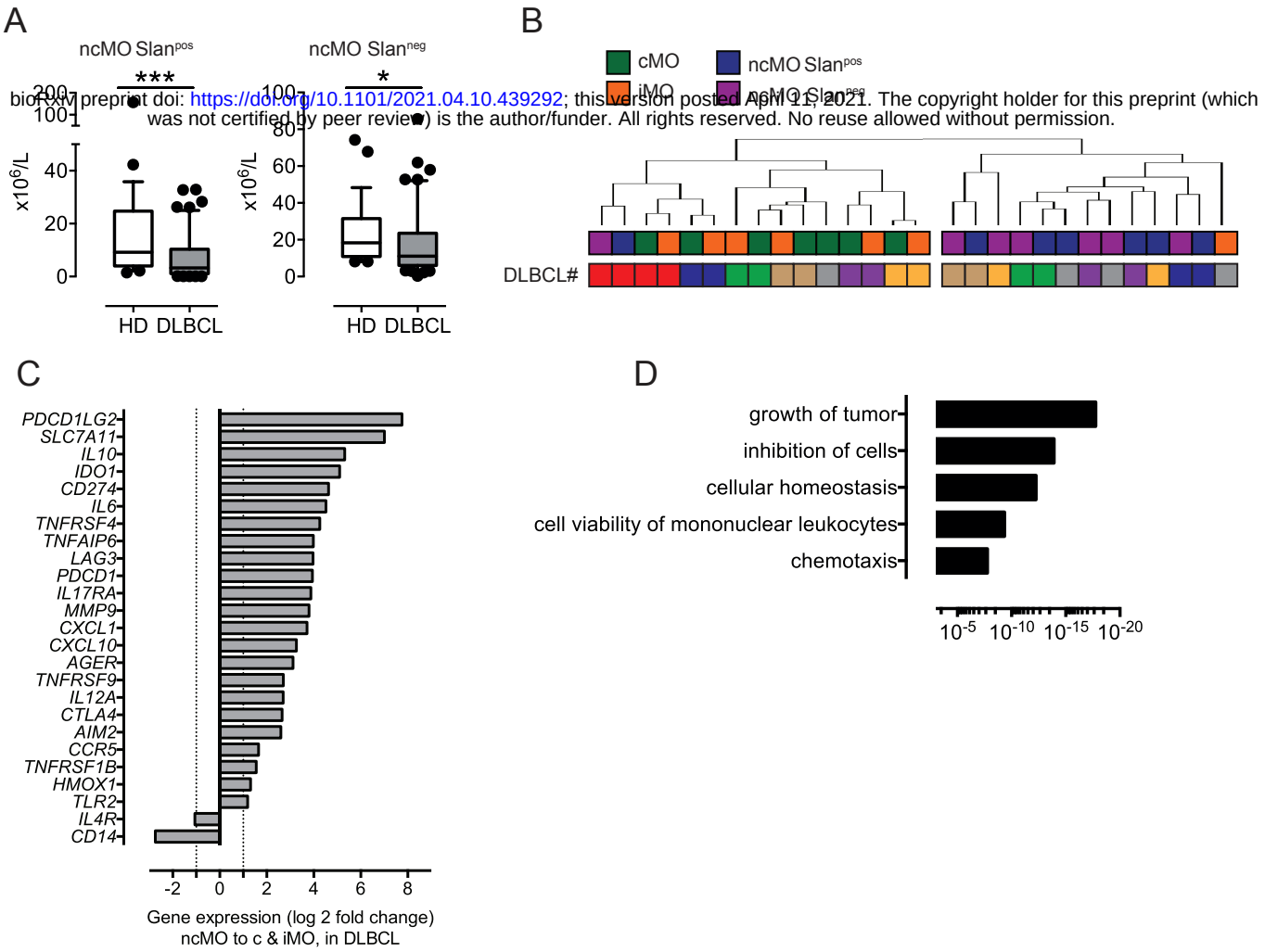

Figure 3

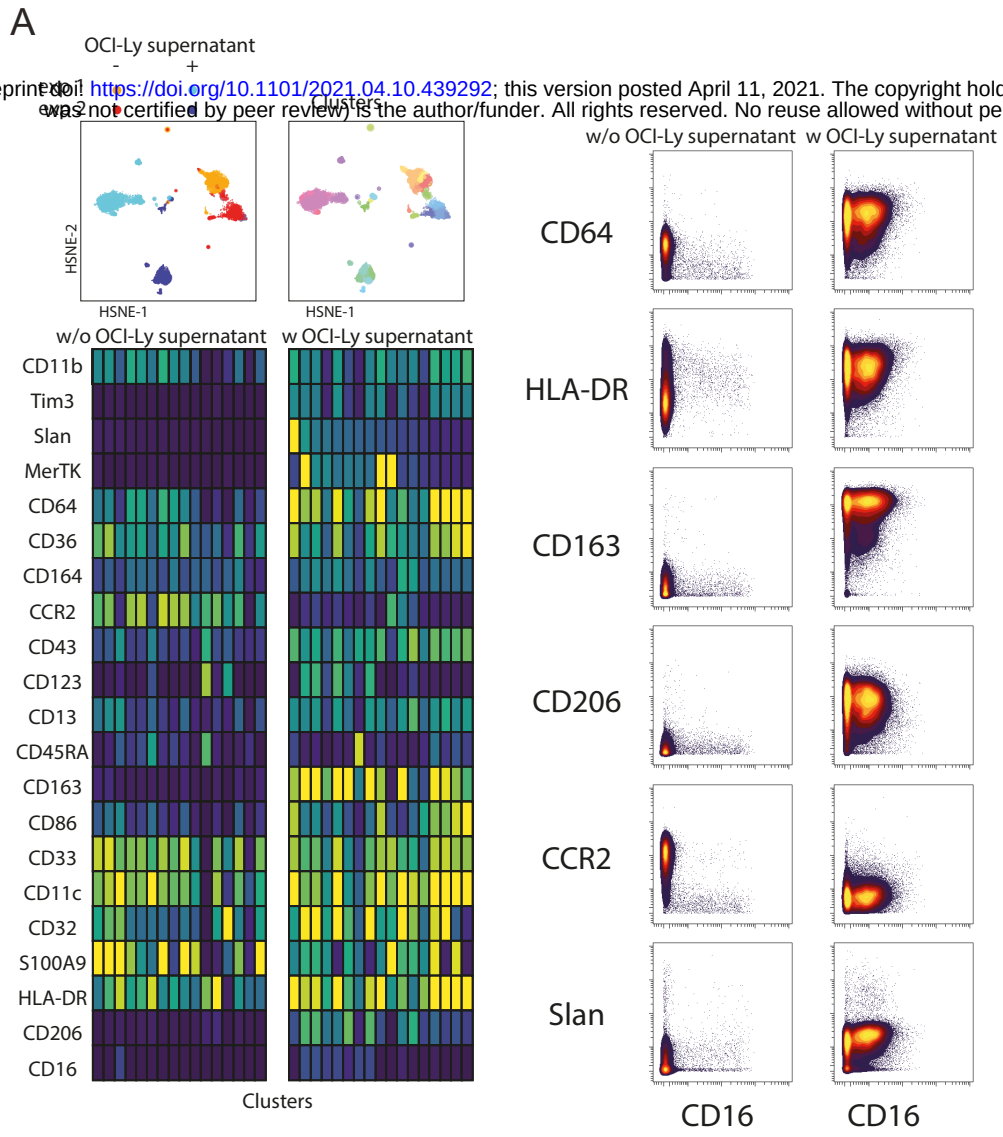

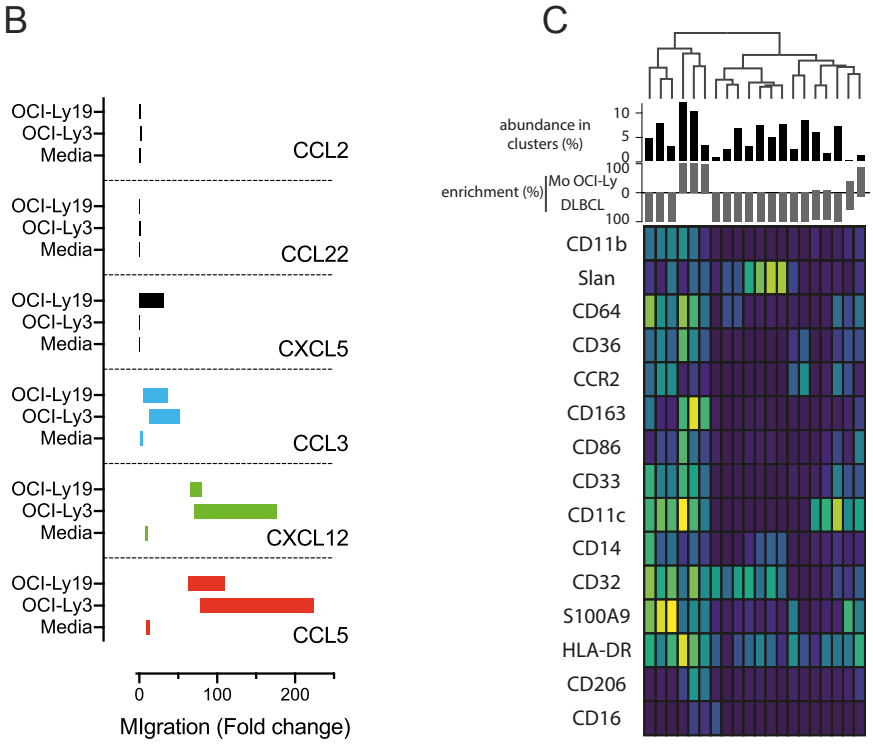

Figure 4

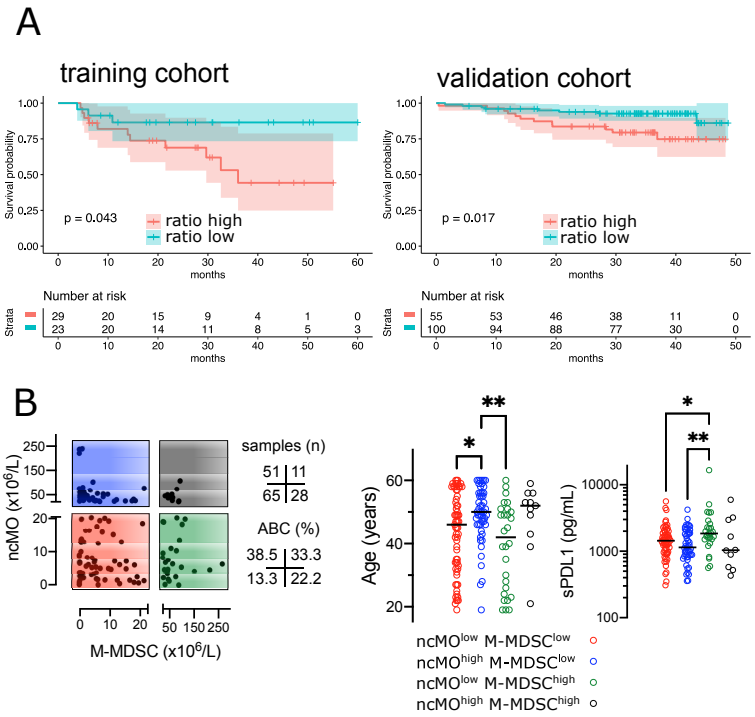

Figure 5